# Optimal Planning of CHP-based Microgrids Considering DERs and Demand Response Programs

Saeid Qaeini, Mehrdad S. Nazar
Fac. of Elect. Eng.,
Shahid Beheshti University,A.C.
Tehran, Iran
saeid.qaeini@gmail.com
m_setayesh@sbu.ac.ir

Miadreza Shafie-khah
School of Tech. and Innov.,
University of Vaasa
Vaasa, Finland
mshafiek@univaasa.fi

Gerardo J. Osório
C-MAST, University of Beira
Interior, Covilha, Portugal
gjosilva@gmail.com

João P. S. Catalão
Faculty of Engineering of the
University of Porto and
INESC TEC, Porto, Portugal
catalao@fe.up.pt

***Abstract*—This work addresses a stochastic framework for optimal operation and long-term expansion planning of combined heat and power based microgrid as a part of an active distributing system. The microgrid utilizes renewable energy sources, electricity and heat generation units, energy storage systems, and demand response programs. The proposed model determines the optimal location and capacity of the electrical and thermal facilities, and it considers the impact of renewable energy sources and demand response on the expansion-planning problem. A stochastic mixed-integer linear programming formulation is utilized to minimize the investment and operation costs of system for five years. To evaluate the effectiveness of the proposed model, the algorithm is assessed for the 9-bus system and the 33-bus IEEE test systems. The results demonstrate that the utilization of the proposed algorithm reduces the operational cost and increases system revenues.**

***Keywords—Microgrid, Combined heat and power, Renewable energy, Distributed generation, Expansion planning, Demand response.***

## I. INTRODUCTION

Nowadays, power system planners consider the distributed energy resources (DERs) in their expansion planning exercises to increase the reliability of their system and reduce the emission of pollutants [1].

MicroGrids (MGs) are considered as a key solution for integrating the renewable and intermittent distributed energy resources, Combined Heat and Power (CHP) systems, Thermal energy Storage Systems (TSSs), and Electricity Storage Systems (ESSs) [2]. Many studies have been accomplished on the planning and operational scheduling of MGs and some of them have investigated the expansion-planning problem.

Ref. [3] has proposed a model for sitting and sizing of ESSs in MGs, which utilizes renewable energy sources and responsive loads. The planning model includes the uncertainties of parameters such as renewable energy, islanding feature of MG, and load variations. A Mixed Integer Linear Programming (MILP) optimization approach was used to solve the model. The results showed that the utilization of ESS and Demand Response Programs (DRPs) reduced the total cost.

Ref. [4] has proposed a bi-level optimization algorithm for optimal expansion planning of a multi-zone MG that consisted of distributed energy resources and combined cooling, heat and power systems. A multi-stage heuristic solution was utilized to solve the nonlinear problem.

Ref. [5] presented a day-ahead Energy Management System (EMS) to minimize the operation cost and increase the reliability of an MG that utilized CHP units, ESSs, and auxiliary boiler to meet thermal and electrical demands in both grid-connected and islanded modes.

Ref. [6] has proposed a two-level optimization algorithm for the optimal operation of an Active Distribution System (ADS). The case study demonstrated that the benefit of energy hub increased about 185% and the operational cost decreased about 82.2%.

Ref. [7] has presented a scenario-based planning model for an off-grid MG considering electricity, heating, and cooling energy sources and demands. The proposed method minimized the total cost and Carbon Dioxide ($CO_2$) emissions.

Ref. [8] has proposed a bi-level optimization problem for scheduling a grid-connected MG. The Time of use (TOU) based DRP was employed. The simulation results depicted that the proposed method by using the DRP reduced the operational and environmental costs up to 2% and 12.45%, respectively.

Ref. [9] has presented an algorithm for expansion planning of ADS that included Active MGs (AMG) and sold its surplus power to the upward network. The Active Distribution System (ADS) includes energy sources such as CHPs, Wind Turbines (WT), PhotoVoltaic (PV) systems, ESSs, and boilers. The introduced method reduced the total expansion planning costs for two case studies about 44.04% and 11.82% with respect to the uncoordinated bidding of AMGs/DRPs costs, respectively.

The present paper utilizes a Stochastic Mixed-Integer Linear Programming (SMILP) method to consider the uncertainties of the expansion-planning problem and optimize the investment and operational costs of the system.

The main contributions of this paper can be summarized as follows:

- The proposed model uses a SMILP framework for the optimal expansion planning and operation of energy networks of a CHP-based MG,
- The uncertainty of market price, electrical and thermal loads, renewable generations uncertainties are considered,
- The impact of consumers' participation in DRPs on MG design and operation plan is determined.

The rest of this paper is organized as follows: Section 2, the model of the problem is described and the details of the proposed approach are introduced. Section 3 the simulation results are addressed and discussed. Finally, the conclusion is drawn in Section 4.

## II. PROBLEM DESCRIPTION AND MODELING

The energy resource candidates consist of CHP units, PVs, WTs, ESSs, TSSs, and gas-fired boilers. The CHP units and boilers supply heat demands through a heat transmission system. The proposed algorithm is illustrated in Fig. 1.

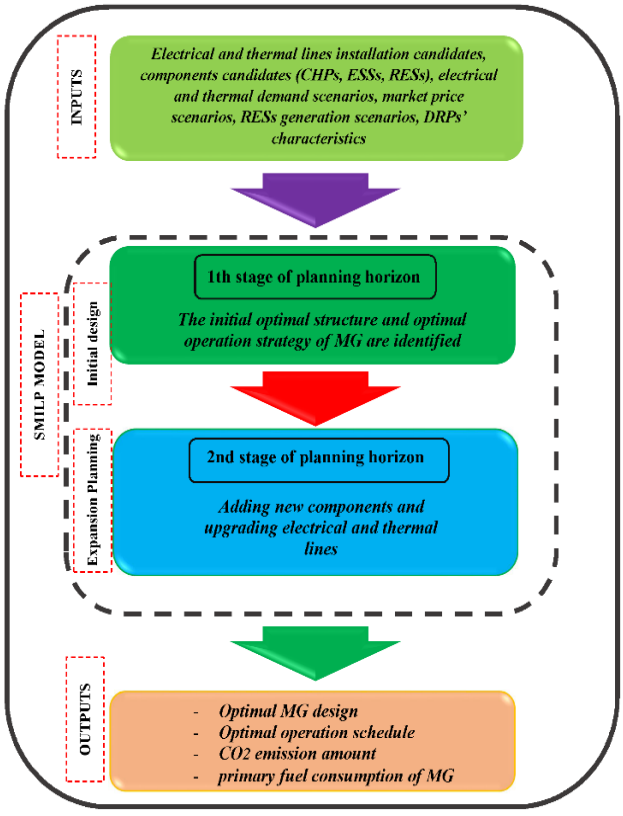


Fig. 1. Proposed MG expansion planning and operation algorithm.

The uncertainties of the planning and operational variables are the electrical and thermal demands, the market prices, and output power of PV and WT units [9].

## A. Wind Turbine Model

The relationship between wind speed and WT power production can be modelled as follows [10]:

$$P_w = \begin{cases} 0 & v \le v_{ci} \\ k_1 v + k_2 & v_{ci} \le v \le v_r \\ P_r & v_r \le v \le v_{ci} \\ 0 & v \ge v_{co} \end{cases} \qquad (1)$$

$$k_1 = \frac{p_r}{v_r - v_{ci}}; \quad k_2 = -k_1 \times v_{ci}$$

Where, $v$ is the wind speed, $v_c$ is the cut-in speed, $v_r$ is the rated speed, $v_o$ is cut-out speed, $P_r$ is rated power of WT.

## B. Demand Response

In this work, a price-based demand response (PBDR) model is employed. The load elasticity is defined as [11]:

$$e_{lv,ls} = \frac{\Delta P_{lv}^D / P_{lv}^{D,0}}{\Delta \pi_{ls} / \pi_{ls}^0} \begin{cases} e_{lv,ls} \le 0, & if \quad lv = ls \\ e_{lv,ls} \ge 0, & if \quad lv \ne ls \end{cases} \qquad (2)$$

Where, $ls$ and $lv$ are load levels, $P_{lv}^{D,0}$ is the baseload, $\Delta P_{lv}^D$ is the load after implementing of PBDR, $\pi_{ls}^0$ is the base electricity price, $\Delta\pi_{ls}$ is the price change after PBDR.

The load shifting can be presented as (3) [11]:

$$P_{lv}^D = P_{lv}^{D,0} \times \left( 1 + e_{lv,lv} \times \frac{\left[\pi_{lv} - \pi_{lv}^0\right]}{\pi_{lv}^0} + \sum_{\substack{ls=1 \\ ls \ne lv}}^{N_{ls}} e_{lv,ls} \times \frac{\left[\pi_{ls} - \pi_{ls}^0\right]}{\pi_{ls}^0} \right). \qquad (3)$$

The PBDR cost can be formulated as (4) [12]:

$$COST_{lv}^{PBDR} = \pi_{lv}^0 P_{lv}^{D,0} - (\pi_{lv}^0 + \Delta\pi_{lv}) P_{lv}^D . \qquad (4)$$

## C. Objective Function

The objective function minimizes the total cost of the facilities installation and operation in the planning period and is formulated as (5):

$$obj \Rightarrow Min \quad Cost = C_{Investment} + C_{Operarion} \qquad (5)$$

*The Cost* term is expressed as (6):

$$Cost = \sum_{t=1}^{T} \frac{1}{(1+d)^t} \left\{ \begin{array}{l} \left[ \begin{array}{l} \sum_{i=1}^{N_i} \sum_{\substack{j=1 \\ (j \ne i)}}^{N_j} CRF_{Ln_k} . C_{INV}^{Ln_k}(i,j,t) . L_{ij} . \lambda_{ij,t}^{Ln_k} + \\ \sum_{i=1}^{N_i} \sum_{\substack{j=1 \\ (j \ne i)}}^{N_j} CRF_{P} . C_{INV}^{P}(i,j,t) . L_{ij} . \lambda_{ij,t}^{P} + \\ \sum_{m=1}^{NCHP} CRF_{CHP_k} . C_{INV}^{CHP_k}(m,t) + \sum_{B=1}^{NB} CRF_{Bo_k} . C_{INV}^{Bo_k}(B,t) + \\ \sum_{n=1}^{NPV} CRF_{PV} . C_{INV}^{PV}(n,t) . P_{nst}^{pv} . A_n + \sum_{w=1}^{Nw} CRF_{WT} . C_{INV}^{WT}(w,t) + \\ \sum_{u=1}^{Nu} CRF_{ES} . C_{INV}^{ES}(u,t) + \sum_{z=1}^{Nz} CRF_{TS} . C_{INV}^{TS}(z,t) \end{array} \right] + \\ \sum_{S=1}^{N_S} Prob(s) . \sum_{lv=1}^{LV} \left[ \begin{array}{l} \sum_{m=1}^{NCHP} (C_O^{CHP} . P_{m,t,lv,s}^{CHP} + F_{m,t,lv,s}^{CHP} . \pi_{t,lv,s}^{F}) + \\ \sum_{B=1}^{NB} (C_O^{Bo} . Q_{B,t,lv,s}^{Bo} + F_{B,t,lv,s}^{Bo} . \pi_{t,lv,s}^{F}) + \\ \sum_{n=1}^{NPV} C_O^{PV} . P_{n,t,lv,s}^{PV} . A_n + \sum_{w=1}^{Nw} C_O^{WT} . P_{w,t,lv,s}^{WT} + \\ \sum_{u=1}^{Nu} C_O^{ES} . (P_{u,t,lv,s}^{CH,ES} + P_{u,t,lv,s}^{DCH,ES}) + \\ \sum_{z=1}^{Nz} C_O^{TS} . (Q_{z,t,lv,s}^{CH,TS} + Q_{z,t,lv,s}^{DCH,TS}) + \\ (P_{t,lv,s}^{Buy} - P_{t,lv,s}^{Sel}) . \pi_{t,lv,s}^{E} + \\ COST_{t,lv,s}^{PBDR} \end{array} \right] \times SD \end{array} \right\} \qquad (6)$$

In (6), the $i$ and $j$ indices are bus indices, and $m$, $n$, $w$, $B$, $u$, and $z$ are indices of CHP, PV, WT, boiler, ESS and TSS units, respectively. The $N_i$ and $N_j$ parameters are the numbers of buses, and $N_m$, $N_n$, $N_w$, $N_B$, $N_u$, $N_u$, and $N_z$ are numbers of CHP, PV, WT, boiler, ESS and TSS units, respectively. The $t$ parameter is the planning stage index and $ls$ and $lv$ are load level indices.

Further, the $C_{INV}^{Ln_k}, C_{INV}^{P}, C_{INV}^{CHP_k}, C_{INV}^{WT}, C_{INV}^{BO_k}, C_{INV}^{ES}, C_{INV}^{TS}$ parameters are investment cost of an electrical line of type $k$, thermal pipeline, CHP unit type $k$, WT, boiler type $k$, electric and thermal storages, respectively. The $\lambda_{ij,t}^{Ln_k}$, $\lambda_{ij,t}^{P}$ parameters are equal to one if the type $k$ electric line is installed between buses $i$ and $j$, and the pipeline is installed between buses $i$ and $j$.

The $L_{ij}$ parameter is the distance between $i$ and $j$ load points, respectively. The $C_O^{CHP}, C_O^{WT}, C_O^{PV}, C_O^{Bo}, C_O^{ES}, C_O^{TS}$ parameter are CHP unit, WT, PV array, boiler, and electric and thermal storage operation costs, respectively.

*Prob(s)* is the probability of scenario $s$. $P_{i,t,lv,s}^{CHP}, P_{i.t,lv,s}^{PV}, P_{i.t,lv,s}^{WT}$ are the produced power by CHP unit, PV and WT at bus $i$, stage planning $t$, load level $lv$ and scenario $s$.

$Q_{m.t,lv,s}^{CHP}, Q_{m.t,lv,s}^{BO}$ are the thermal power that are produced by CHP units and boilers, respectively. $F_{i,t,lv,s}^{CHP}$, $F_{i,t,lv,s}^{BO}$ are the amount of fuel which is consumed by CHP units and boilers, respectively. $P_{i,t,lv,s}^{CH,ES}$, $P_{i,t,lv,s}^{DCH,ES}$ are the amount of charged and discharged electric power by ESS unit, respectively.

$Q_{i,t,lv,s}^{CH,TS}$, $Q_{i,t,lv,s}^{DCH,TS}$ are the amount of charged/discharged thermal power by TSS, respectively.

$P^{Buy}_{t,lv,s}$, $P^{Sel}_{t,lv,s}$ are the exchanged power with the upstream network, respectively. $\pi^{F}_{t,lv,s}$, $\pi^{E}_{t,lv,s}$ are fuel and electricity price, respectively.

*SD* is the planning days. To calculate the annualized capital cost, the capital recovery factor (CRF) of each equipment is used. In (7) CRF is expressed, where *dr* is the interest rate and *n* is the lifetime of each component in years, respectively.

$$CRF = \frac{dr(1+\mathrm{dr})^{n}}{(1+\mathrm{dr})^{n}-1} \tag{7}$$

### D. Constraints

The optimization model considers the following equality and inequality constraints:

- Feasible operating region of a CHP plant [4]:

$$\alpha^{th}_{CHP,i} \times P^{CHP}_{m,i,t} + \beta^{th}_{CHP,i} \times Q^{CHP}_{m,i,t} \geq \gamma^{th}_{CHP,i} \quad ,th \in \{1,2,3\} \tag{8}$$

Where, $\alpha^{th}_{CHP,i}, \beta^{th}_{CHP,i}, \gamma^{th}_{CHP,i}$ are the coefficients of heat-power feasible region for the CHP unit.

- Energy balance constraints: The electrical and thermal power balance for each site in each year, load level, and each scenario:

$$P^{Buy}_{t,lv,s} + \sum_{m} P^{CHP}_{m,t,lv,s} + \sum_{n} P^{PV}_{n,t,lv,s} + \sum_{w} P^{WT}_{w,t,lv,s} + \sum_{u} P^{DCH,ES}_{u,t,lv,s} = P^{D}_{i,t,lv,s} + P^{Sel}_{t,lv,s} + \sum_{u} P^{CH,ES}_{i,t,lv,s}; \qquad \forall i,t,lv,s \tag{9}$$

$$Q^{CHP}_{i,t,lv,s} + Q^{Bo}_{i,t,lv,s} + Q^{DCH,TS}_{i,t,lv,s} = Q^{D}_{t,lv,s} + Q^{CH,TS}_{i,t,lv,s} + \sum_{\forall j, j \neq i} Q_{ij,t,lv,s}.(1-\delta_h.L_{ij}). \quad \forall i,t,lv,s \tag{10}$$

Where, in (9) and (10), $P^{D}_{i,t,lv,s}$, $Q^{D}_{i,t,lv,s}$ are electric and thermal demands of bus *i*. $\delta_h$ in (9) is percentage loss along the thermal pipelines per length unit ($km^{-1}$).

- DC power flow equation and electrical power flow limits:

$$P^{CHP}_{i,t,lv,s} + P^{PV}_{i,t,lv,s} + P^{WT}_{i,t,lv,s} + P^{DCH,ES}_{i,t,lv,s} - P^{CH,ES}_{i,t,lv,s} + P^{Buy}_{t,lv,s} - P^{Sel}_{t,lv,s} - P^{D}_{i,t,lv,s} = \sum_{\substack{j=1 \\ j \neq i}}^{Nj} Pflow_{ij,t,,lv,s} \quad ,\forall i,t,lv,s \tag{11}$$

$$Pflow_{ij,t,lv,s} = \frac{1}{X_{ij}} \times (\delta_{i,t,lv,s} - \delta_{j,t,lv,s}) \quad ,\forall i,j,t,lv,s \tag{12}$$

$$\left| Pflow_{ij,t,lv,s} \right| \leq Pflow^{\max} \quad ,\forall i,j,t,lv,s \tag{13}$$

Where, *Pflow* is the power flow between buses *i* and *j*, and $Pflow^{max}$ is the maximum limit of the transferring power. $\delta_{i,t,lv,s}$ and $\delta_{j,t,lv,s}$ are voltage angles of buses *i* and *j*.

- Limit of power generations for CHP:

$$P^{CHP}_{min} \leq P^{CHP}_{i,t,lv,s} \leq P^{CHP}_{\max}, \quad \forall i,t,lv,s \tag{14}$$

Where, $P^{CHP}_{min}$ and $P^{CHP}_{max}$ are the minimum/maximum active power of the CHP unit connected to bus *i*, respectively.

- Limit of the thermal power of boilers:

$$Q^{Bo}_{min} \leq Q^{Bo}_{i,t,lv,s} \leq Q^{Bo}_{\max}, \quad \forall i,t,lv,s \tag{15}$$

Where, $Q^{CHP}_{min}$ and $Q^{CHP}_{max}$ are the minimum/maximum output of the boiler connected to bus *i*, respectively.

- Limit of the thermal flow of pipeline:

$$Q^{P,\min}_{ij} \leq Q^{p}_{ij,t,lv,s} \leq Q^{P,\max}_{ij} \quad \forall i,j,t,lv,s \tag{16}$$

$$Q^{P}_{ij,t,lv,s} \leq Cap^{P}_{ij} \quad \forall i,j,t,lv,s \tag{17}$$

Where, $Cap^{P}_{ij}$ is the maximum capacity of the installed pipeline.

- The constraint of thermal flow that is transferred from the site *i* to site *j* can be written as (18):

$$xh_{ij} + xh_{ji} \leq 1 \quad \forall t,lv,s \tag{18}$$

The ESS constraints include storage battery limit and maximum charge and discharge rate of battery and these constraints are presented in (19), (20), and (21), respectively. The *X* and *Y* variables are the binary variables that present the discharge and charge of electric storage, respectively.

$$P^{ES}_{i,t,lv,s} \leq Cap^{ES}, \quad \forall i,t,lv,s \tag{19}$$

$$P^{CH,ES}_{i,t,lv} \leq P^{ES}_{RCH}.X_{t,lv,s} \quad \forall i,t,lv,s \;,\; X \in \{0,1\} \tag{20}$$

$$P^{DCH,ES}_{i,t,lv} \leq P^{ES}_{RDCH}.Y_{t,lv,s} \quad \forall i,t,lv,s \;,\; Y \in \{0,1\} \tag{21}$$

The ESS cannot charge/discharge at the same time in each load level:

$$X_{t,lv,s} + Y_{t,lv,s} \leq 1 \quad \forall t,lv,s \tag{22}$$

Where, $Cap^{ES}$ is the ESS unit capacity. $P^{ES}_{RCH}$ and $P^{ES}_{RDCH}$ are the charge/discharge rate of the ESS unit, respectively.

- The constraints of thermal storage system include the limits of thermal storage:

$$Q^{TS}_{i,t,lv,s} \leq Cap^{TS}, \quad \forall i,t,lv,s \tag{23}$$

$$Q^{CH,TS}_{i,t,lv} \leq Q^{TS}_{RCH}.Xh_{t,lv,s} \quad \forall i,t,lv,s \;,\; Xh \in \{0,1\} \tag{24}$$

$$Q^{DCH,TS}_{i,t,lv} \leq Q^{TS}_{RDCH}.Yh_{t,lv,s} \quad \forall i,t,lv,s \;,\; Yh \in \{0,1\} \tag{25}$$

$$Xh_{t,lv,s} + Yh_{t,lv,s} \leq 1 \quad \forall t,lv,s \tag{26}$$

Where, $Cap^{TS}$ is the TSS unit capacity. $Q^{TS}_{RCH}$ and $Q^{TS}_{RDCH}$ are charge and discharge rate of TSS unit, respectively.

The constraints of the PV system are presented in (27) and (28) [12]:

$$P^{PV}_{i,t,lv,s} \leq It_{t,lv,s}.\eta_{PV}.A_i, \quad \forall i,t,lv,s \tag{27}$$

$$P^{PV}_{i,t,lv,s} \leq P^{PV}_{rat}.A_i, \quad \forall i,t,lv,s \tag{28}$$

Where, $It_{t,lv,s}$ is the solar irradiance ($W/m^2$), $\eta_{PV}$ is the PV arrays efficiency, and $A_i$ is the surface of arrays at bus *i*. $P^{PV}_{rat}$ is the rated capacity of the PV panel ($kW/m^2$).

- The constraint of WT generation:

$$P^{WT}_{i,t,lv,s} \leq P^{WT}_{max}, \quad \forall i,t,lv,s \tag{29}$$

Where, $P^{WT}_{max}$ is the maximum active power of the WT connected to bus *i*.

- Limits of power exchange with the upstream network:

$$P^{Buy}_{t,lv,s} \leq P^{EXCH}_{\max} \quad \forall t,lv,s \tag{30}$$

$$P^{Sel}_{t,lv,s} \leq P^{EXCH}_{\max} \quad \forall t,lv,s \tag{31}$$

Where, $P^{EXCH}_{max}$ is the maximum active power that it could be exchanged with the upstream network.

- DRP operation constraints:

$$\Delta P^{\min}_{DR} \leq \Delta P^{D}_{lv} \leq \Delta P^{\max}_{DR} \tag{32}$$

Where, $\Delta P^{min}_{DR}$ and $\Delta P^{min}_{DR}$ are the minimum/maximum load change in DRP, respectively.

## III. Simulation and Results

The 9-bus and IEEE 33-bus test systems are considered to assess the model [13]. The planning horizon is 5 years. The technical and cost information of CHP units, ESSs and PV units are presented in [4]. MMUs stands for Million Monetary

Units. The rated capacity of WT is 35 kW. The boilers and TSS characteristics are available in [14]. The interest rate is considered 12.5%.

The value of $\delta_h$ for calculation of thermal network is 18%. It is assumed that 1000 $m^2$ (150 kW) space exists in the defined load points for PV arrays installation.

The candidate conductors are introduced in [13]. Three-time intervals are defined in TOU-DRP: from 00:00h to 07:00h as valley period, 8:00h and from 15:00h to 16:00h, and 22:00h to 23:00h off-peak period, and 9:00h to 14:00h, and 17:00h to 21:00h as the peak period. Further, it is considered that the price in the valley and peak periods are decreased and increased by 25% with respect to the base case, respectively. Moreover, self and cross elasticities are considered as -0.2 and 0.01, respectively.

The price of natural gas is assumed 0.03 MUs/$m^3$ at all times. Fig. 2, and Fig. 3 depict forecasted solar and power generation and upward market price, respectively. The load growth rate is considered 3%. The algorithm codes were developed in GAMS and MATLAB. There are 5 scenarios:

- Scenario 1: The MG purchases electricity from the utility grid to supply its loads. Only boilers are used to supply the heat loads.
- Scenario 2: The microgrid installs CHP systems and thermal transmission pipelines. Further, the MG can sell its surplus electricity to the upward utility grid.
- Scenario 3: The microgrid implements the second scenario alternatives and it installs ESSs.
- Scenario 4: The microgrid implements the third scenario alternatives and it installs PV arrays and WTs.
- Scenario 5: The microgrid implements the fourth scenario alternatives and it implements DRPs.

### *A. 9-Bus Test System*

The 9-bus system is depicted in Fig. 4. Table I. shows the results of five considered scenarios for the 9-bus system. All of the scenarios lead to a similar electrical topology. Further, the thermal system topology is the same as the electrical system topology for all of the scenarios.

In the second scenario, two 1210 kW gas turbines are installed in buses 5 and 7, respectively, and three 1300 kW gas-fired boilers are installed in buses 4, 5, and 6, respectively. In the third scenario, one 1210 kW gas turbine bus 4, one 1300 kW boiler in bus 6, two 1630 kW boilers in buses 6 and 8, and two 4560 kW boiler in buses 2 and 7 are installed; and also, batteries are installed in buses 3, 4, 5, and 7; and thermal storage is installed in bus 2.

In the fourth scenario, one 1210 kW gas turbine is installed in bus 7. Two 1300 kW gas-fired boilers and one 1630 kW are installed in buses 3, 4, and 9. ESSs are installed in buses 2, 6, 7, and 9; and a TSS is installed in bus 6.

The RESs are installed in predetermined buses. The optimal MG for the fifth year of scenario 5 is shown in Fig. 5. The electrical and thermal power dispatch of fifth year of fourth scenario is illustrated in Fig. 6 and Fig. 7, respectively. By assessing Table I, it is obvious that the amount of $CO_2$ emission and primary energy consumption are reduced from scenarios 2 to 4 due to adding ESSs, TSSs and RESs.

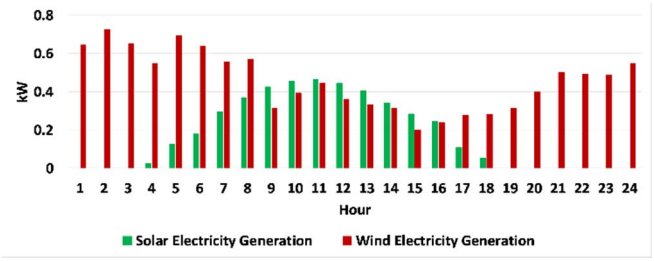


Fig. 2. Forecasted solar and wind power generation.

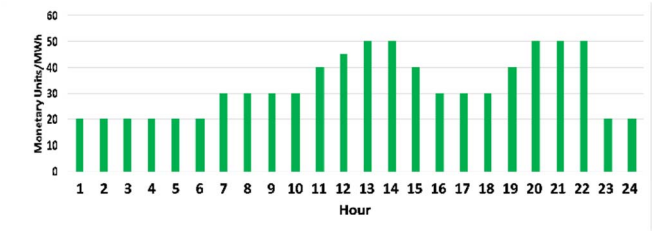


Fig. 3. Forecasted upward market price.

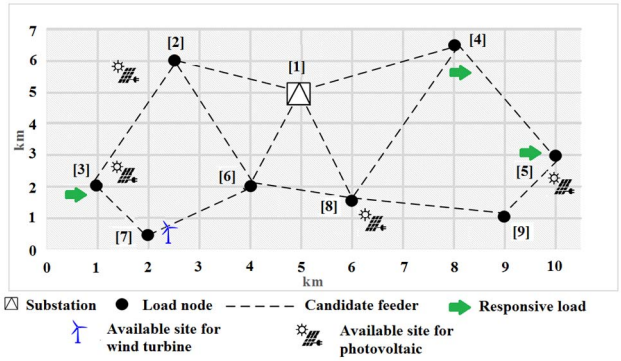


Fig. 4. The 9-bus MG.

In the fifth scenario by implementing DRP, and because of that the reduction in peak load, the selling electricity to the upward network is increased; thus, the operation cost and objective function are reduced 22.6% and 6.6% compared to the base case, respectively.

In Fig. 6 and Fig. 7, the behavior of DRP and ESSs are presented. The ESSs are charged during off-peak times, in which the market price is lower than peak times, and discharged during peak periods.

Thus, they effectively participate in the increase of MG total profit. Fig. 8 shows the thermal flow through pipelines among buses.

TABLE I. OPTIMIZATION RESULTS FOR THE 9-BUS MG.

| | Scenario | | | | |
|---|---|---|---|---|---|
| | **1** | **2** | **3** | **4** | **5** |
| **Investment Costs (MMUs)** | 0.870 | 4.221 | 2.167 | 2.812 | 5.061 |
| **Operation Costs (MMUs)** | 4.390 | 3.847 | 4.335 | 4.278 | 3.396 |
| **Objective Function (MMUs)** | 4.500 | 4.412 | 4.924 | 4.819 | 4.203 |
| **Primary Energy Consumption (TOE)** | 9986.2 | 26102.2 | 18649.3 | 18936.6 | 30681.3 |
| **$CO_2$ emission (tons)** | 91559.8 | 99341.6 | 95057.2 | 93444.3 | 100853 |

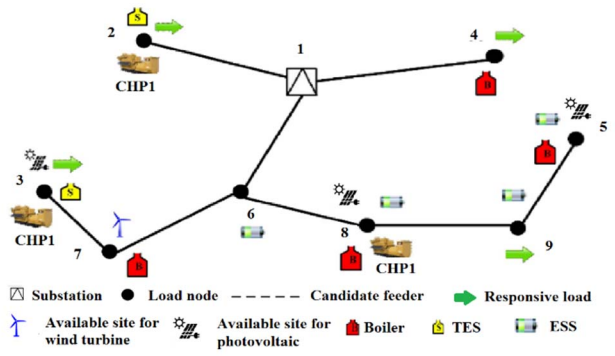


Fig. 5. The optimal plan of the 9-bus MG (Scenario 5).

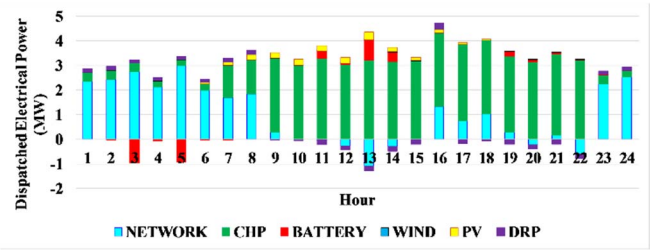


Fig. 6. The electrical power dispatch of the 9-bus MG in scenario 5.

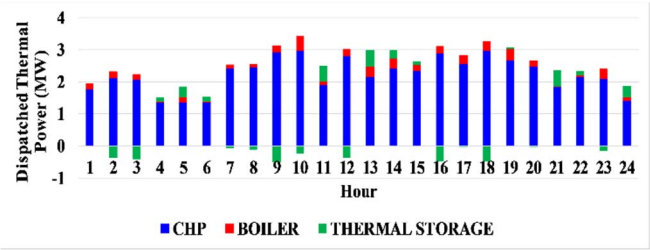


Fig. 7. The thermal power dispatch of the 9-bus MG in scenario 5.

### B. 33-Bus Test System

Fig. 9 illustrates the radial 33-bus MG [15]. The demand curves are similar to the 9-bus MG load curves; but the peak of electrical and thermal loads are 11145 kW and 8358 kW, respectively. Table II shows the results of introducing the five considered scenarios for 33-bus MG.

In the second scenario, one of 1210 kW and two of 5200 kW gas turbines are installed in buses 8, 24, and 30, respectively. Five boilers of 1300 kW are installed in buses 5, 7, 16, 18, and 19. Eleven boilers of 1630 kW are installed in buses 2, 3, 9, 12, 13, 14, 15, 21, 25, 29, and 32. Two 1950 kW boilers are installed in buses 8 and 31.

In the third scenario, two 1210 kW and two of 3515 kW gas turbines are installed in buses 8, 24, 29, and 31, respectively. Eight 1300 kW boilers are installed in buses 17, 20, 23, 24, 25, 26, 30, and 32; and 1630 kW, 1950 kW, and 2600 kW boilers are installed in buses 4, 8, and 14, respectively. The ESSs are installed in buses 4, 5, 25, 28, 30, and 31.

The TSSs are installed in buses 12, 25, 30, 31, and 32. The optimal MG for the fifth year of the fifth scenario is shown in Fig. 10. The electrical and thermal power dispatches of the fifth year of the fourth Scenario are illustrated in Fig. 11 and Fig. 12, respectively.

Fig. 13 shows the thermal flow through pipelines among buses. All scenarios lead to a similar electrical topology. The thermal system topology is the same as the electrical system topology for all scenarios.

Table II shows that in 33-bus case the reductions of operation cost and objective function in scenario 5 are 26.14% and 13.5% in comparison with the base case, respectively.

In scenario 4, one 3515 kW gas turbine is installed in bus 24. Two 1300 kW gas-fired boilers are installed in buses 10 and 20. Five 1630 kW boilers are installed in buses 4, 7, 12, 25, and 31.

Six 1950 kW boilers are installed in buses 8, 9, 13, 22, 28, and 30. Four 2600 kW boilers are installed in buses 15, 17, 19, and 29. One 3900 kW boiler is installed in bus 33. Electric storages are installed in buses 10, 18, 23, 26, 27, and 28. One thermal storage is installed in bus 23.

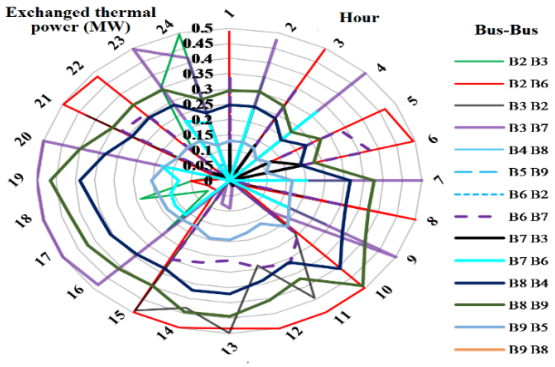


Fig. 8. Thermal flows exchange among buses in the 9-bus MG (Scenario 5).

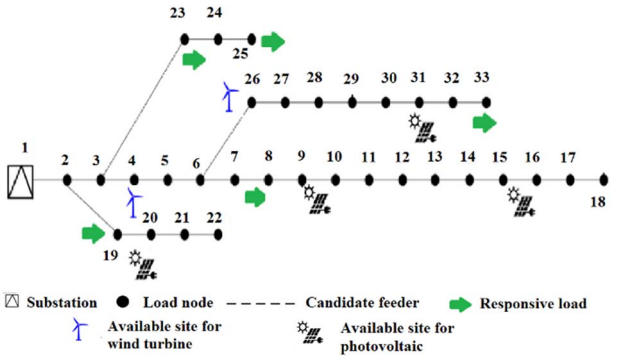


Fig. 9. The 33-bus MG.

## IV. Conclusion

This work proposed a model for optimal expansion planning and operation scheduling of an MG, which was a part of an ADS. In five scenarios, different energy sources were considered in MG such as CHP units, PV arrays, WTs, EESs, and gas-fired boilers. It was considered that the MG transacted electricity with the upward wholesale market. The effect of RES and DRP were investigated on the issue of MG design, operation, and expansion planning. The model utilized a SMILP formulation to minimize the investment and operational cost of a 5-year planning horizon.

TABLE II. Optimization Results for 33-Bus MG.

| | Scenario | | | | |
|---|---|---|---|---|---|
| | 1 | 2 | 3 | 4 | 5 |
| **Total investment Cost (MMUs)** | 2.362 | 10.880 | 11.510 | 6.770 | 13.050 |
| **Operation cost (MMUs)** | 14.000 | 11.937 | 12.670 | 14.260 | 10.340 |
| **Objective Function (MMUs)** | 14.300 | 13.320 | 14.320 | 15.400 | 12.370 |
| **Primary energy consumption (TOE)** | 31996.0 | 130783.5 | 72704.3 | 58339.9 | 125750.0 |
| **$CO_2$ emission (tons)** | 292450 | 337178 | 279760 | 297674 | 355629 |

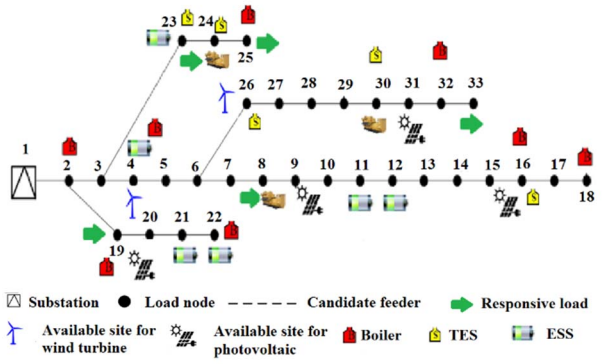


Fig. 10. The optimal plan of 33-bus MG (Scenario 5).

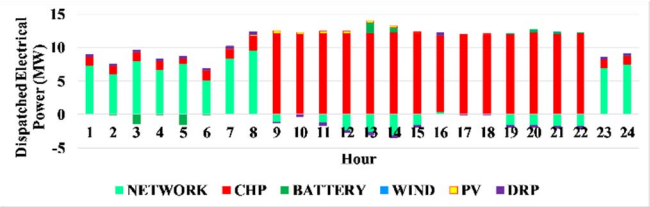


Fig. 11. The electrical power dispatch of the 33-bus MG in scenario 5.

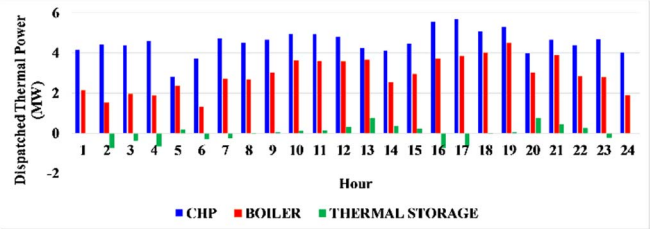


Fig. 12. The thermal power dispatch of the 33-bus MG in scenario 5.

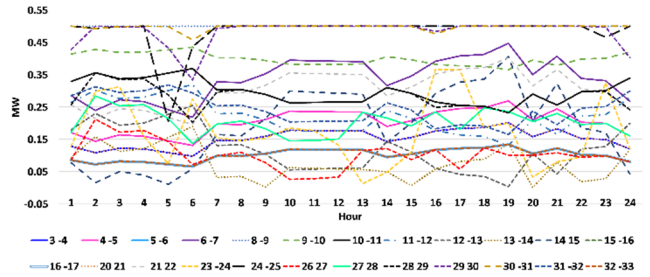


Fig. 13. Thermal flows exchanged among buses in the 33-bus MG (Scenario 5).

The results showed that the total investment and operation costs reduced about 6.6% and 13.49% for the 9-bus and 33-bus test systems. The results demonstrated that utilizing CHP units alongside the thermal transmission system reduces primary energy consumption in MG, and utilizing ESSs and RES, and DRP increases the MG profitability.

## ACKNOWLEDGMENT

J.P.S. Catalão acknowledges the support by FEDER funds through COMPETE 2020 and by Portuguese funds through FCT, under POCI-01-0145-FEDER-029803 (02/SAICT/2017). G.J. Osório acknowledges the support by UIDB/00151/2020 research unit (C-MAST) funded by FCT.

## REFERENCES

[1] M. Quashie, F. Bouffard, C. Marnay, R. Jassim, and G. Joós, "On bilevel planning of advanced microgrids," *International Journal of Electrical Power & Energy Systems,* vol. 96, pp. 422-431, 2018.

[2] M. Alipour, B. Mohammadi-Ivatloo, and K. Zare, "Stochastic scheduling of renewable and CHP-based microgrids," *IEEE Transactions on Industrial Informatics,* vol. 11, no. 5, pp. 1049-1058, 2015.

[3] M. Biazar Ghadikolaei, M. Shahabi, and T. Barforoushi, "Expansion planning of energy storages in microgrid under uncertainties and demand response," *International Transactions on Electrical Energy Systems,* p. 12110, 2019.

[4] F. Varasteh, M. S. Nazar, A. Heidari, M. Shafie-khah, and J. P. Catalão, "Distributed energy resource and network expansion planning of a CCHP based active microgrid considering demand response programs," *Energy,* vol. 172, pp. 79-105, 2019.

[5] P. Firouzmakan, R.-A. Hooshmand, M. Bornapour, and A. Khodabakhshian, "A comprehensive stochastic energy management system of micro-CHP units, renewable energy sources and storage systems in microgrids considering demand response programs," *Renewable and Sustainable Energy Reviews,* vol. 108, pp. 355-368, 2019.

[6] A. Bostan, M. S. Nazar, M. Shafie-khah, and J. P. Catalão, "Optimal Scheduling of Distribution Systems considering Multiple Downward Energy Hubs and Demand Response Programs," *Energy,* p. 116349, 2019.

[7] A. Ehsan and Q. Yang, "Scenario-based investment planning of isolated multi-energy microgrids considering electricity, heating and cooling demand," *Applied energy,* vol. 235, pp. 1277-1288, 2019.

[8] H. Hosseinnia and B. Tousi, "Optimal operation of DG-based micro grid (MG) by considering demand response program (DRP)," *Electric Power Systems Research,* vol. 167, pp. 252-260, 2019.

[9] S. Qaeini, M. S. Nazar, M. Yousefian, A. Heidari, M. Shafie-khah, and J. Catalao, "Optimal Expansion Planning of Active Distribution System Considering Coordinated Bidding of Downward Active Microgrids and Demand Response Providers," *IET Renewable Power Generation,* vol. 13, pp. 1291-1303, 2019.

[10] M. S. Borujeni, A. A. Foroud, and A. Dideban, "Accurate modeling of uncertainties based on their dynamics analysis in microgrid planning," *Solar Energy,* vol. 155, pp. 419-433, 2017.

[11] L. Ju, Z. Tan, J. Yuan, Q. Tan, H. Li, and F. Dong, "A bi-level stochastic scheduling optimization model for a virtual power plant connected to a wind–photovoltaic–energy storage system considering the uncertainty and demand response," *Applied Energy,* vol. 171, pp. 184-199, 2016.

[12] E. D. Mehleri, H. Sarimveis, N. C. Markatos, and L. G. Papageorgiou, "Optimal design and operation of distributed energy systems: Application to Greek residential sector," *Renewable Energy,* vol. 51, pp. 331-342, 2013.

[13] M. S. Nazar, A. R. Sadegh, and A. Heidari, "Optimal Microgrid Operational Planning Considering Distributed Energy Resources," in *Microgrid Architectures, Control and Protection Methods*: Springer, 2020, pp. 491-507.

[14] S. Sanaye and N. Khakpaay, "Simultaneous use of MRM (maximum rectangle method) and optimization methods in determining nominal capacity of gas engines in CCHP (combined cooling, heating and power) systems," *Energy,* vol. 72, pp. 145-158, 2014.

[15] M. Kia, M.S. Nazar, M.S. Sepasian, A. Heidari, and J.P.S. Catalão, "New framework for optimal scheduling of combined heat and power with electric and thermal storage systems considering industrial customers inter-zonal power exchanges", *Energy*,vol. 138, no. 1, pp. 1006-1015, 2017.